AIAA Paper No. 95-1234

On The Isolation Of Science Payloads From Spacecraft Vibrations

W. Keith Belvin, Dean W. Sparks
Lucas G. Horta, and Kenny B. Elliott

NASA Langley Research Center

Presented At The 36th AIAA/ASME/ASCE/AHS/ASC Structures, Structural Dynamics, and Materials Conference
New Orleans, LA

April 1995

National Aeronautics and
Space Administration

Langley Research Center
Hampton, Virginia 23681-0001

ON THE ISOLATION OF SCIENCE PAYLOADS FROM SPACECRAFT VIBRATIONS

W. Keith Belvin *, Dean W. Sparks†,
Lucas G. Horta‡, and Kenny B. Elliott‡

NASA Langley Research Center, Hampton, VA 23681-0001

Abstract

The remote sensing of the Earth's features from space requires precision pointing of scientific instruments. To this end, the NASA Langley Research Center has been involved in developing numerous controlled structures technologies. This paper describes one of the more promising technologies for minimizing pointing jitter, namely, payload isolation. The application of passive and active payload mounts for attenuation of pointing jitter of the EOS AM-1 spacecraft is discussed. In addition, analysis and ground tests to validate the performance of isolation mounts using a scaled dynamics model of the EOS AM-1 spacecraft are presented.

Introduction

The EOS AM-1 mission involves remote sensing of the Earth's environment for an improved understanding of environmental change. Five major instrument systems (payloads) are being integrated onto the EOS AM-1 spacecraft[1]. The science instruments must be precisely pointed to obtain the spatial resolution required for the science data. Unfortunately, vibrations cause variations in the angular orientation of the science instrument with respect to Earth. Pointing jitter, defined as the peak-to-peak variation in the actual pointing direction within a given time window, is associated with short intervals of time for which the attitude control system (ACS) has little effect. Conversely, pointing stability refers to longer intervals of time in which the ACS can reduce the peak-to-peak angular variations of the spacecraft. Pointing jitter/stability is a primary design driver for remote sensing spacecraft.

Studies of the EOS AM-1 spacecraft's pointing jitter/stability have indicated the potential for low pointing margins on some key instruments due to instrument flexibility and rigid-body platform motion. These studies simulate the dynamic response caused by spacecraft and instrument disturbances. The disturbance energy propagates through the spacecraft and is transmitted to the scientific payloads through the mounts that join the payload to the spacecraft. Often times, this mounting hardware consists of some form of kinematic mount.

Kinematic mounts are used to isolate spacecraft thermal distortions from the science payloads. They transmit no rotational torques and only 1 (z), 2 (x, z), or 3 (x, y, z) translation forces between the spacecraft and the payload. To improve the pointing jitter performance of scientific instruments, the use of isolation mounts is proposed herein. The goal is to make the isolation mounts interchangeable with a normal kinematic mount. The isolation mounts would help isolate both thermal distortions and vibratory disturbances.

Since vibration isolation is extensively reported in the literature, a review of pertinent work is appropriate. Payload isolation has been studied for a number of different applications. Isolation of heavy machinery uses primarily passive mounts to prevent motion from migrating to the surrounding environment. The work discussed in Refs. [2-3] showed approaches for passive and active concepts where the distinguishing factor between active and passive is the need for an external power source. Reference [4] discussed different isolation concepts and an application of both active and passive vibration isolation to a diesel engine. Passive mounts, commonly fabricated from rubber materials, are by far the most commonly used form of isolation for industrial applications. Rubber provides the low stiffness high energy absorption properties required in many industrial applications[5]. A critical aspect of rubber and other elastomeric materials is the variability of the stiffness and loss factor as a function of frequency, temperature, and amplitude of excitation. Sensitivity to temperature, in particular, makes their use unlikely for space operations.

---

* Structures Division, Associate Fellow AIAA.

† Flight Dynamics and Controls Division.

‡ Structures Division, Member AIAA.

In the automotive industry, engine mounts which were initially used only to support the engine, are now being used as a means to reduce the disturbances which degrade the ride quality of vehicles. Shock isolation is also a concern in applications such as aircraft landing gears and automobiles. Reference [6] proposed a shock isolator using a strut filled with silicon oil where the oil compressibility serves as a mechanical spring and the damping is achieved by moving the oil through an orifice. A similar concept was used successfully with the Hubble Space Telescope reaction wheels[7].

Generally, the isolation problem takes one of two forms: (a) a machine or an instrument which must be isolated from disturbances originated in its support structure; (b) a machine or instrument produces disturbances which must be prevented from migrating to the supporting structure. Reference [8] summarizes a number of issues associated with vibration isolation in terms of concepts, materials, and control approaches. Space applications, in particular the International Space Station Alpha (ISSA), have prompted a renewed interest in vibration isolation because of the unique quiescent environment that space provides. Early in the program, ISSA recognized the importance of isolating instruments on the station to prevent unwanted vibrations from propagating to other instruments. Studies were initiated to examine isolation concepts for instrument racks which would provide 6 degrees-of-freedom of load carrying capability. Some of the initial approaches, discussed in Refs. [9-11], are based on magnetic suspension systems. Another promising concept called the active rack isolation system (ARIS) is described in Ref. [12].

In addition to isolation concepts, the literature also shows the importance of analyzing isolation system performance. Reference [13] discussed physical limitations and an impedance matching approach for the design of various isolation concepts. Reference [14] presented the recent development of general models for isolation systems in terms of mobility as opposed to impedance. Frequency domain analysis based on a four-pole mobility representation is used to develop the equations of motion and to identify key design parameters. An important property of any isolation system is the effectiveness in reducing the transmission of forces or velocities across the interfaces. Most of the work dealing with isolation mounts is presented in terms of single mount concepts. However, it is common practice to use multiple support points. It has been shown that the effectiveness of an isolation system cannot be accurately determined using a single mount analysis[16].

As indicated above, most isolation system concepts require significant changes to normal or baseline payload mounting systems. In addition, the isolation of payloads with multiple support points has not been adequately investigated. Since all instruments and equipment modules are interfaced to the EOS AM-1 spacecraft by kinematic mounts, the use of payload isolator mounts is considered in this study. A key aspect of the isolator mount design is to make them interchangeable with a normal (baseline) mount. Thus, passive/active isolation mounts can be incorporated into the spacecraft at the preliminary design review (PDR) or even as late as the critical design review (CDR) with very little cost and schedule impact. In addition to the above design goals, it is highly desirable to develop an isolator mount which can withstand launch-loads without special caging or other operational modes. This objective is to simplify the design, to reduce command and control operations and ultimately to reduce cost.

This paper explores the use of passive and active payload mounts to help isolate science payloads from spacecraft disturbances. First, pointing jitter of the EOS AM-1 spacecraft is described to show the need for payload isolation. Next, payload kinematic mounts are described along with design guidelines for replacement isolator mounts. A dynamics testbed used to study technological issues associated with spacecraft pointing control and to ground test payload isolation systems is described. The development of simulation models for the EOS AM-1 spacecraft and the dynamics testbed with payload isolators is presented. Then, simulation results for the EOS AM-1 spacecraft with passive and active isolator mounts are shown. Ground tests results for piezoelectric actuated payload mounts are also presented. Finally, some concluding remarks and plans for continued development of spacecraft payload isolation mounts are given.

Pointing Jitter of EOS AM-1 Spacecraft Payloads

The five instrument systems selected for flight onboard the EOS AM-1 spacecraft are[1]:

1. The Advanced Spaceborne Thermal Emission and Reflection (ASTER) radiometer. ASTER consists of three radiometers; visible and near infrared (VNIR), short-wave infrared (SWIR), and thermal infrared (TIR).
2. The Clouds and Earth's Radiant Energy System (CERES) scanning radiometers.
3. The Multi-Angle Imaging SpectroRadiometer (MISR)
4. The Moderate-Resolution Imaging Spectroradiometer (MODIS)
5. And the Measurements of Pollution In The Troposphere (MOPITT) correlation spectrometer.

Each of these instruments has specific pointing requirements which are derived from the desired spatial resolution of the science data and various instrument and orbit parameters. During the spacecraft design, dynamic response analyses are made to ascertain the pointing stability and jitter at each instrument's boresight location. Under a collaborative agreement between the NASA Goddard Space Flight Center (GSFC) and the NASA Langley Research Center (LaRC), the preliminary design review (PDR) disturbance, structural dynamics, and attitude control models were used to predict the dynamic response of the EOS AM-1 spacecraft. These jitter simulations were made with an efficient sparse matrix code called PLATSIM[16].

In the PDR jitter assessment of the EOS AM-1 spacecraft, twelve disturbance events were used to determine the probable jitter amplitude. These disturbances include the CERES biaxial scan, MISR calibration, MODIS scan mirror imbalance, MOPITT scan operations, ASTER-SWIR pointing, ASTER-TIR chopper mechanism, ASTER-VNIR pointing, cryocoolers on MOPITT, ASTER-SWIR, and ASTER-TIR, reaction wheel assembly (RWA), and the solar array drive (SAD). For brevity, jitter amplitudes for only two instruments is presented herein; ASTER-SWIR and MISR. (The three ASTER radiometers will be referred to simply as SWIR, VNIR, and TIR in the remainder of the text.)

A graphical presentation of the pointing jitter simulation results is given in Figure 1. The pointing requirements are given in arc-seconds. The root-sum-square (RSS) total of the individual disturbances shows that the pointing requirements are only marginally met. The primary disturbance events contributing to jitter were the VNIR pointing, the SWIR cryocooler, the CERES biaxial scan, and the SAD. The VNIR and SWIR Cryocooler disturbances are of a high frequency content whereas the CERES and SAD primarily excited rigid-body and solar array response. Hence, pointing performance enhancements must address not only pointing stability (low frequency response), but also pointing jitter (high frequency response). The next section describes a method to lower the amplitude of payload jitter.

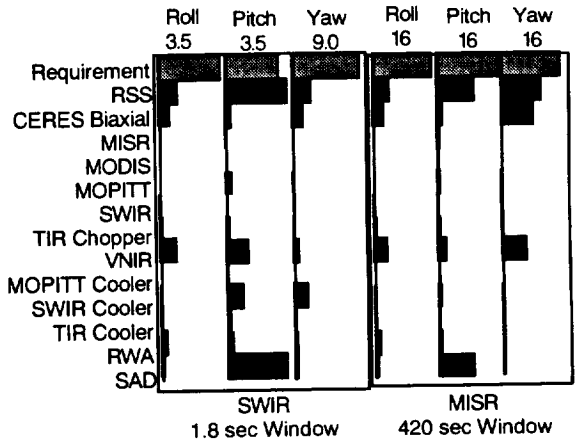

Figure 1. Instrument pointing jitter/stability in arc-seconds

Payload To Spacecraft Isolation Mounts

To reduce disturbance induced vibrations of spacecraft payloads, passive and active isolation methods have been evaluated. Since all instruments and equipment modules are interfaced to the EOS AM-1 spacecraft by kinematic mounts, the use of replacement isolator mounts is considered. The payload mounts are good candidates for isolation because they directly transmit the disturbances to/from the instruments.

Kinematic mounts isolate local rotations from propagating into the science instrument payloads. They transmit no rotational torques. Hence, a properly designed isolator mount need only provide translational motion compensation to isolate the attached payload. Figure 2 shows typical kinematic mounts used on the EOS AM-1 spacecraft. These mounts use bearings to prevent torque transfer. In other spacecraft designs, flexure mounts have been used to reduce torque transfer. Flexure based kinematic mounts use sections of low cross-sectional inertia to minimize bending/torsion stiffness. It must also be noted that the term "kinematic" mount is often a misnomer. In order for a mounting system to be kinematic, it must be structurally determinate. However, most science payloads and equipment modules on-board the EOS AM-1 spacecraft use four or more mounts to attach to the spacecraft bus. Thus, the mounting system is usually indeterminate and not a true "kinematic" interface.

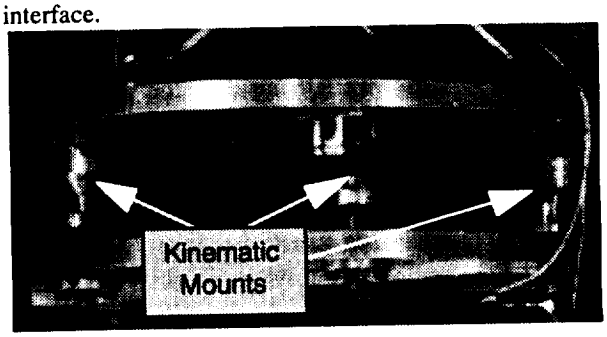

Figure 2. EOS AM-1 spacecraft kinematic mounts

A key aspect of the isolator mount design undertaken in this study is to make them interchangeable with a normal (baseline) mount. This will provide the spacecraft designer flexibility to adapt to unanticipated dynamic requirements prior to launch. Jitter prediction is quite sensitive to modeling assumptions and disturbance frequency content. By making the isolator mounts interchangeable with baseline mounts, the designer would have the ability to replace one or more mounts if jitter predictions show low margins. Thus, passive/active isolation mounts can be incorporated into the spacecraft design at PDR or even as late as the CDR with very little cost and schedule impact.

In addition to the above design goals, it is highly desirable to develop an isolator mount which can withstand launch-loads without special caging or other operational modes. This objective is to simplify the design, to reduce command and control operations and ultimately to reduce cost. The present technology development seeks to determine how many mounts must be isolators, what feedback (or feedforward) sensors for an active system are most efficient, and how to design simple yet effective controllers for virtually autonomous operation. A dynamics testbed has been assembled to provide answers to these and other technology issues associated with spacecraft pointing control. The next section describes this testbed.

LaRC EOS Dynamics Testbed

The EOS Dynamics Testbed is the fifth in a sequence of laboratory models, developed at the NASA Langley Research Center, used to enhance the understanding of how to model, control, and design spacecraft and their subsystems. This testbed was created to develop and test precision pointing technologies associated with medium sized earth science and remote sensing platforms; such as, the EOS AM-1 spacecraft. The latest version of the testbed was designed to emulate the on-orbit dynamic behavior of the EOS AM-1 spacecraft[17].

Figure 3 shows the testbed which consists of a simulated spacecraft bus structure, two flexible appendages which represent the solar array and the high-gain antenna, dummy instrument and spacecraft subsystem masses, a suspension system to provide near free-free boundary conditions, three gimbaled instrument payloads, and instrumentation to quantify the dynamic response. The following paragraphs provide a description of the parts and characteristics of the testbed relevant to this study.

The simulated spacecraft bus is a truss structure built-up from 10 inch cubical bays. The geometry of the bus is approximately the same geometry as that of the EOS AM-1 spacecraft. However, due to limitations of the suspension system, the combined bus, payloads, and subsystems weight is approximately 1/10 the on-orbit weight of the EOS AM-1 spacecraft. Weight constraints produced a testbed with mass and stiffness characteristics scaling as 1/10 of full-scale, while geometry and frequency characteristics scale as unity. The first system bus natural frequency is 23 Hz. The testbed is suspended, from five cables, approximately 65 ft. below an over-head platform using pneumatic suspension devices. Near orbital boundary conditions are achieved since all six "rigid-body" mode frequencies are below 0.3 Hz.

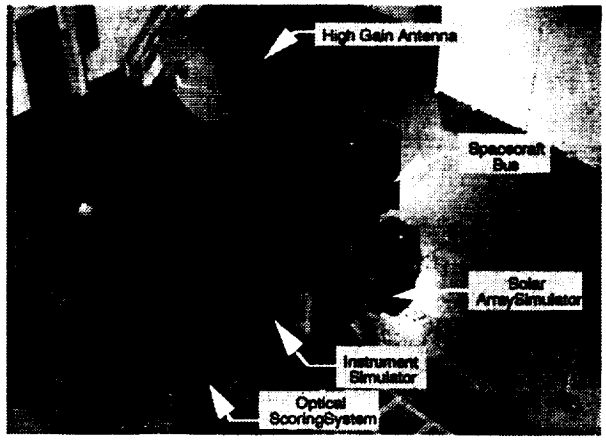

Figure 3. LaRC EOS Dynamics Testbed

Three instrument payloads simulate the actions of pointing or low-bandwidth scanning payloads. All three payloads are two axes gimbal devices. The payloads are positioned on the testbed at three locations representative of the EOS AM-1 spacecraft's TIR, MISR, and CERES instrument locations. Each is capable of pointing to within 2 arc-seconds with a bandwidth of approximately 8 Hz. One gimbal is rigidly attached to the bus (CERES location). Another gimbal is attached to the bus through a kinematic mounting system similar to that used on EOS AM-1 (TIR location). The third gimbal is mounted to the bus via isolator mounts that use piezoelectric actuators (MISR location).

Accelerometers are used to quantify the dynamics at the instrument/bus interface, and an optical scoring system (OSS) is used to quantify the pointing performance of the payloads. The accelerometers are arranged such that four are mounted on the gimbaled instrument interface plate, in line with each mount as

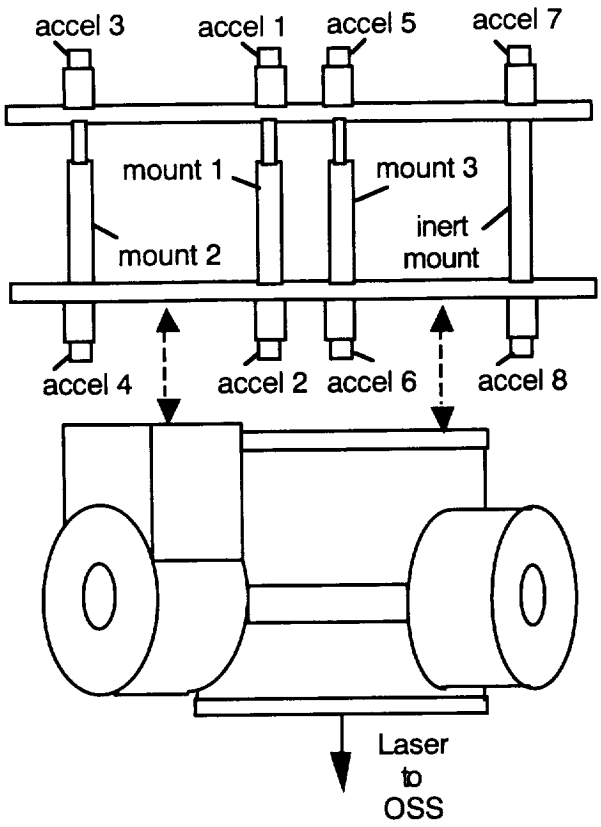

Figure 4. Schematic of payload active isolator mounts on testbed

shown in Fig. 4. An equal number of accelerometers are placed on the testbed interface plate, in line with each strut. The accelerometers have a resolution on the order of 10 micro-g's with a bandwidth of 150 Hz. The optical measurement system is used to measure roll and pitch angular displacement at the boresight of the instrument payloads. These devices have a resolution of 0.2 arc-sec. and a bandwidth of 100 Hz.

Figure 5 shows a photograph of an instrument payload attached to the testbed with isolation mounts. Three of these mounts are commercial piezoelectric stack actuators, made by Polytec-PI, Inc., of Waldbronn, Germany. The fourth mount is a solid aluminum tube. Each of the piezoelectric actuators consists of a stack of individual piezoceramic disks encased in a stainless steel tube. When voltage is applied to each disk in the stack, they expand or contract in their longitudinal direction. By stacking the disks, a cumulative effect of the expansions and contractions can be exploited. Table 1 lists some of the

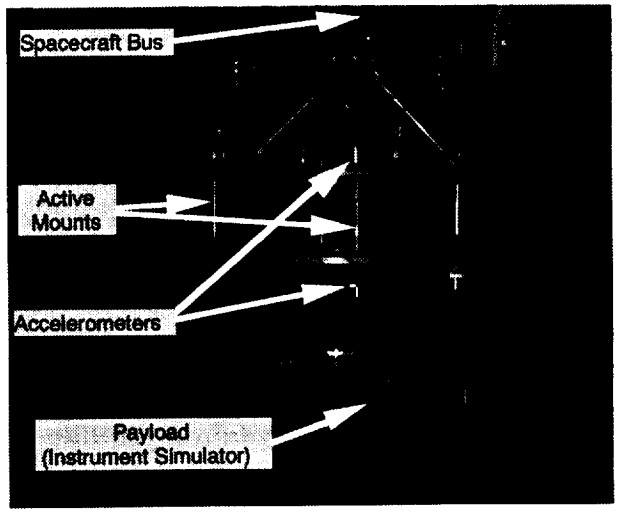

Figure 5. Payload with active isolation mounts on testbed

pertinent characteristics of the piezoelectric devices used in this study [18].

Each piezoelectric actuator is instrumented with a strain gage sensor mounted on its internal piezoceramic stack to measure the total expansion and contraction. The actuators are driven by a 3-channel Polytec-PI P-865.10 amplifier, capable of up to 100 V and 30 W output per channel. For these specific tests, the piezoelectric actuators are operated in the range of +/- 50 volts, to achieve up to 20 microns in expansion and contraction. A built-in servo loop controller is used to help counter the hysteresis inherent in the piezoelectric actuators. This controller, when active, takes the internal strain gage signals and adjusts the command signals for each actuator so that the resulting expansions and contractions are within 0.5% of the desired amounts.

The procedure used for developing simulation models of this testbed and of the EOS AM-1 spacecraft is given in the next section.

Table 1. Piezoelectric actuator parameters

Model Number	P-845.37
Expansion at 100 Volts	40 microns
Max. Pushing Force	300 lb.
Stiffness (k_e)	3.8258 E+05 lb/in
Nominal Length	3.2677 in
Resonant Frequency	9000 Hz

Modeling of Spacecraft With Isolator Mounts

To simulate the dynamic response of structural systems with embedded actuators (isolator mounts), special care must be taken to include the effects of local deformations and actuator dynamics. The following sections describe the approach used to develop analysis models for this study.

Efficient Finite Element Modeling

To begin the modeling process, a standard normal mode NASTRAN Finite Element Model (FEM) analysis was conducted. This analysis provided the structural eigenvalues and eigenvectors. Then, for each isolator mount, a static displacement vector was computed. The static vectors result from opposing loads being applied at each end of the mount. Subsequently, the static vectors were used to form a matrix of Ritz vectors. The combination of eigenvectors and Ritz vectors are used in the simulation models as shown in the following.

The system equations and physical output equations can be written as

$$M\ddot{r} + Kr = Eu \tag{1a}$$

$$\begin{bmatrix} y_L \\ y_S \\ y_A \end{bmatrix} = \begin{bmatrix} H_L & 0 \\ H_S & 0 \\ 0 & H_A \end{bmatrix} \begin{bmatrix} r \\ \ddot{r} \end{bmatrix} \tag{1b}$$

where M K and E are the mass, stiffness and influence matrices, respectively, and r and u are the physical displacement and input vectors, respectively. The output vector consists of the following: y_L , which represents payload rotations (arc-sec); y_S, the strain (in/in) in each piezoelectric strut; and y_A the outputs of the accelerometers (in/sec^2).

It is often necessary to reduce the size of FEM models using modal reduction. However, retaining only eigenvectors in the model reduction process can result in very poor accuracy because the local deformations across the actuator are usually not adequately modeled. To improve the accuracy, static "Ritz" vectors can be appended to the eigenvectors during the model reduction[19-20]. However, the fact that these Ritz vectors are not ordinarily orthogonal to the eigenvectors can greatly increase the storage requirements and computational time of the simulation. The procedure below maintains the accuracy and efficiency of finite element modeling of systems with embedded actuators such as isolation mounts.

With the transformation

$$r = \bar{T}z = \begin{bmatrix} T_e & T_o \end{bmatrix} z \tag{2}$$

where T_e is the set of retained eigenvectors, and T_o is the set of Ritz vectors, one vector for each isolator mount. An important step in the current procedure is to make T_o orthogonal with respect to T_e . The vector z is the transformed displacement vector.

By applying the transformation of Eq. (2) to Eq. (1), The system equations can be written as

$$\hat{M}\ddot{z} + \hat{K}z = \hat{E}u \tag{3}$$

where $\hat{M} = \bar{T}^T M \bar{T}$, $\hat{K} = \bar{T}^T K \bar{T}$ and $\hat{E} = \bar{T}^T E$.

Eq. (3) can be written in the first order form given below

$$\begin{bmatrix} \dot{z} \\ \ddot{z} \end{bmatrix} = \begin{bmatrix} 0 & I \\ -\hat{M}^{-1}\hat{K} & 0 \end{bmatrix} \begin{bmatrix} z \\ \dot{z} \end{bmatrix} + \begin{bmatrix} 0 \\ \hat{M}^{-1}\hat{E} \end{bmatrix} u \tag{4}$$

Similarly, Eq. (2) can be substituted into Eq. (1b), resulting in the output equations in the form

$$\begin{bmatrix} y_L \\ y_S \\ y_A \end{bmatrix} = \begin{bmatrix} H_L\bar{T} & 0 \\ H_S\bar{T} & 0 \\ -H_A\bar{T}\hat{M}^{-1}\hat{K} & 0 \end{bmatrix} \begin{bmatrix} z \\ \dot{z} \end{bmatrix} + \begin{bmatrix} 0 \\ 0 \\ H_A\bar{T}\hat{M}^{-1}\hat{E} \end{bmatrix} u \tag{5}$$

By making T_o orthogonal to T_e, the matrices $\hat{M}$ and $\hat{K}$ in Eq. (4) become

$$\hat{M} = \begin{bmatrix} I & 0 \\ 0 & T_o^T M T_o \end{bmatrix} \text{ and } \hat{K} = \begin{bmatrix} \Lambda & 0 \\ 0 & T_o^T K T_o \end{bmatrix} \tag{6}$$

where Λ is a diagonal matrix containing the eigenvalues associated with the normal eigenvectors. In the simulation of the dynamic response, the sparsity of the structural modal equations can be maintained which greatly improves computational efficiency.

NASTRAN routines can be used to extract the matrices Λ, $T_o^T M T_o$, $T_o^T K T_o$ and $\bar{T}$ directly from the FEM. From these, $\hat{M}$, $\hat{K}$ and $\hat{E}$ can be formed as in Eq. (6) and substituted into Eqs . (4) and (5) to produce a linear state space representation of the spacecraft with isolator mounts.

Inclusion of Actuator Dynamics

The governing equation for piezoelectric actuators used here has been taken from Ref. [21]. One can examine a simple representation of the actuator dynamics with the aid of Figure 6.

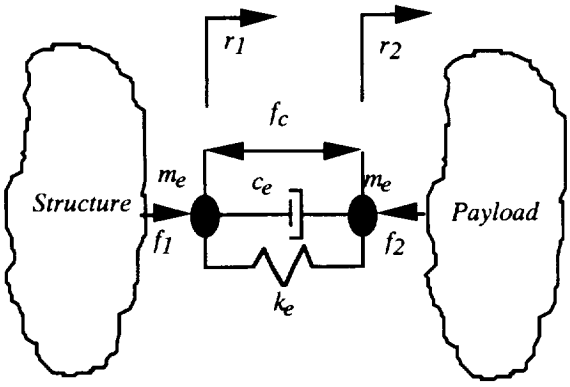

Figure 6. Simplified representation of piezoelectric actuator.

The governing equation is given in the form

$$\begin{bmatrix} m_e & 0 \\ 0 & m_e \end{bmatrix} \begin{Bmatrix} \ddot{r}_1 \\ \ddot{r}_2 \end{Bmatrix} + k_e \begin{bmatrix} 1 & -1 \\ -1 & 1 \end{bmatrix} \begin{Bmatrix} r_1 \\ r_2 \end{Bmatrix} + c_e \begin{bmatrix} 1 & -1 \\ -1 & 1 \end{bmatrix} \begin{Bmatrix} \dot{r}_1 \\ \dot{r}_2 \end{Bmatrix} = \begin{Bmatrix} -f_c \\ f_c \end{Bmatrix} + \begin{Bmatrix} f_1 \\ f_2 \end{Bmatrix} \quad (7)$$

Equivalent properties of the piezoelectric actuator are defined by

$$m_e = m/6;$$
$$k_e = k^d - ch^2$$
$$f_c = chv$$

where the actuator structural mass is m, stiffness is k^d, and c_e is an estimated damping value. For a piezoelectric element, the stiffness k^d is measured with the electric circuit open. Coefficient h is the piezoelectric force/charge constant, c is the capacitance when the actuator is clamped, f_1 and f_2 are applied mechanical forces, and v is the applied voltage. When the actuator is coupled to the structure, the actuator displacements r_1 and r_2 are restricted to move with the structure and the applied forces are constraint forces to keep them together. For simulation, the actuator mass m is considered part of the structural mass.

Polytec-PI power amplifiers are used to drive the piezoelectric actuators. Tests have shown that the amplifier dynamics can be represented as a simple second order system, given here in transfer function form as

$$v(s) = \frac{G\omega^2}{s^2 + 2\omega\zeta s + \omega^2} V(s) \quad (8)$$

with $\omega = 150\,Hz$, $\zeta = 0.7$, $G = 10$, and V is the input voltage to the amplifier.

Model specifics for the LaRC EOS Dynamics Testbed

For the experimental results obtained in this study, the required piezoelectric actuator parameters are taken from Table 1, with k_e = 3.8258 E+05 lb/in, a deformation of $r_2 - r_1$= 20 microns (or 7.87 E-04 in) for a 50 volt input, and ch= 6.025 lb/V.

The signal conditioning for each piezoelectric actuator internal strain gage is controlled by an Analog Devices AD598 chip. The signal conditioning dynamics[22] can be modeled like the amplifier dynamics, using Eq. (7) with $\omega = 100\,Hz$, $\zeta = 0.9$, and $G = 1$.

Simulated and Experimental Payload Isolation Results

The next two sections present simulation results for isolator mounts as applied to the EOS AM-1 spacecraft. Following these sections, experimental isolation data from the LaRC EOS Dynamics Testbed is presented.

EOS AM-1 Spacecraft Simulations

Passive Isolation The EOS AM-1 spacecraft baseline kinematic mounts were designed to provide a stiff interface between the science payloads (weighing 300-600 lbs) and the spacecraft bus. Nominal mount stiffness values range from 1.6 E5 to 1.6 E6 lb/in. In addition, they are designed to withstand launch loads of 4000 to 7500 lbs. These design constraints limit passive isolation system designs to relatively high frequencies. Nevertheless, viscoelastic materials placed in parallel with the baseline mounts can lower the payload pointing jitter.

Finite element models of the EOS AM-1 spacecraft developed for the PDR were modified to include a complex modulus in the kinematic mount stiffnesses. It was assumed that a viscoelastic treatment could produce a loss factor of 0.2 across each of the kinematic mounts. Complex eigenvalue analyses was performed to compute the equivalent modal damping levels of 513 modes. As shown in Figure 7, in the first few modes, the assumed modal damping of 0.0015 is unchanged since no strain energy is stored in the kinematic mounts for the low frequency modes.

The damping data of Figure 7 was used in the spacecraft model to simulate jitter levels for the VNIR disturbance. As shown in Figure 8, jitter was reduced

in all cases with the best performance improvement (30 percent) occurring in pitch for the SWIR and MISR instruments. The limitation of high stiffness and the desire to avoid designs which must be caged during launch severely restricts the performance of a passive isolator. More effective isolation can be achieved with active isolation systems as shown next.

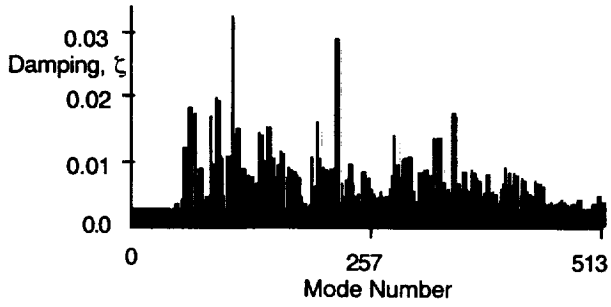

Figure 7. Equivalent modal damping from viscoelastic treatment

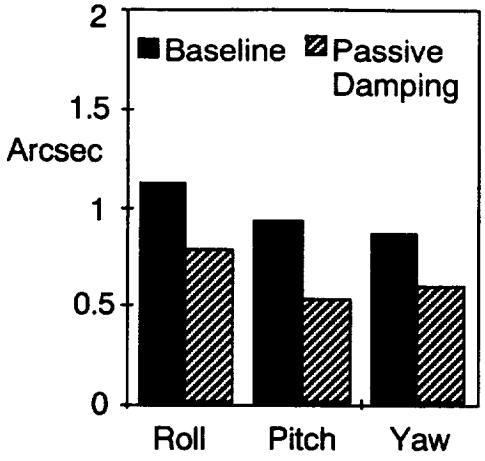

a) SWIR jitter in 1.8 sec window

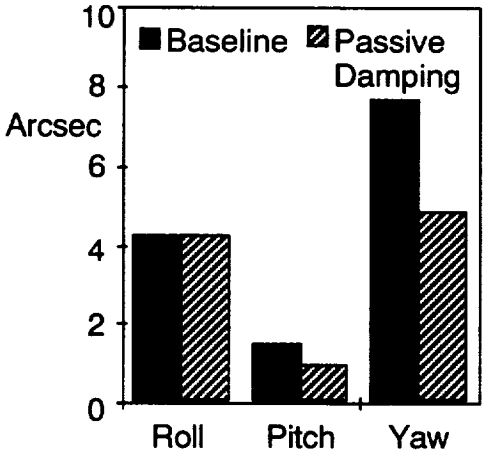

b) MISR jitter in 420 sec window

Figure 8. Jitter response of SWIR and MISR due to VNIR disturbance

Active Isolation Analysis of the EOS AM-1 spacecraft indicated the VNIR disturbance produced about 1 arcsec/1.8 sec. of jitter in all three axes of SWIR. In the simulation model, the SWIR and VNIR mounts were made active by embedding a piezoelectric actuator in series with the kinematic mounts. Strain and strain rate feedback were used to help isolate the VNIR disturbance and the SWIR instrument. Simulations showed a simple low pass filter could significantly lower the pitch and yaw response of SWIR as shown in figure 9. The SWIR roll response is reduced by only 30 percent because there is significant rigid-body motion about the roll axis which cannot be mitigated by the isolation system. As an aside, the MISR instrument response was also reduced by about 10 percent.

The simulations showed that for the EOS AM-1 application, only a 20 micro-inch stroke and less than 15 lbs of force were required by the isolation mounts. These force and stroke levels are easily obtained using commercial piezoelectric stack actuators. Thus isolator mounts, designed to be interchangeable with the baseline kinematic mounts, would provide a viable instrument or disturbance isolation system for EOS class payloads.

The next section describes experimental results from the LaRC EOS Dynamics Testbed using active mounts for payload isolation.

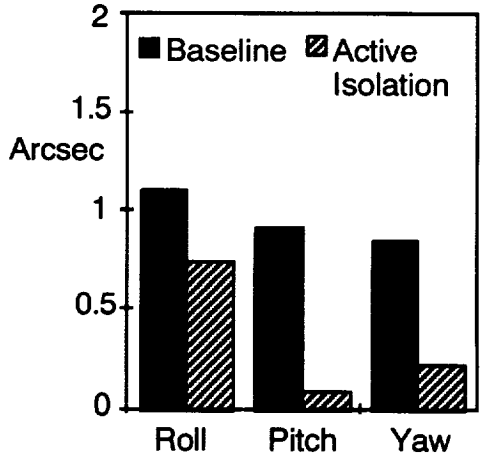

Figure 9. Jitter response of SWIR (1.8 sec.) due to VNIR disturbance with active isolation

EOS Dynamics Testbed Experimental Results

The LaRC EOS Dynamics Testbed has been used for evaluation of various isolation concepts. This section presents payload isolation results using the previously mentioned Polytec-PI devices for the isolation mount actuators.

While the objective of payload isolation is to reduce boresight pointing jitter of the payload, this measurement is not usually available for feedback. Hence the acceleration on the payload side of the isolator mount and the acceleration on the spacecraft bus side of the mount have been selected for feedback control (see Fig. 4). A simple two-zero, two-pole control law was used in conjunction with a bandpass filter in the feedback loop. A second order Butterworth filter was used with break frequencies at 20 and 60 Hz. The controller zeros were each set at 100 rad/s, whereas each controller pole was set to 1 rad/s. The controllers have been implemented digitally at an update rate of 1000 Hz.

The three active isolator mounts that support the payload have been controlled independently. With reference to Fig. 4, typical compensator dynamics for commanding mount #1 using accelerometers #1 and #2 for feedback is shown graphically in Fig. 10. Open-loop (baseline) and closed-loop (isolated) frequency response functions of Accelerometer #2 due to an excitation at the SWIR cryocooler location is shown in Fig. 11 The isolator mount provides significant attenuation at key frequencies. Similar results have also been achieved using mount #3 with accelerometers #5 and #6 as shown in Fig. 12. It is noted that the bandwidth of the isolators is approximately 45 Hz. Above this frequency, the compensator rolls off and the phase delay actually accentuates the response level. To determine the transmissibility across the interface, one can examine the ratio of open-loop acceleration (hard mounted) to closed-loop acceleration (isolated). Fig. 13 shows the transmissibility using mount #3 and accelerometer # 6. These data show the isolation mounts do provide broadband performance.

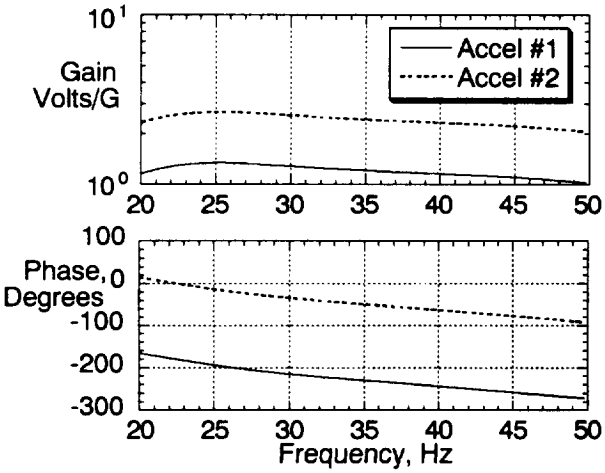

Figure 10. Compensator dynamics

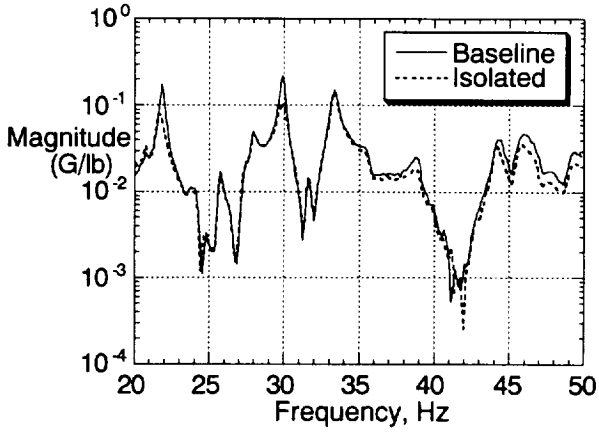

Figure 11. Frequency response of accelerometer # 2

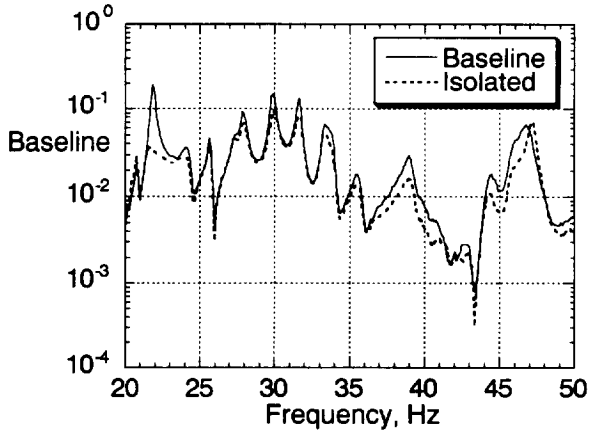

Figure 12. Frequency response of accelerometer # 6

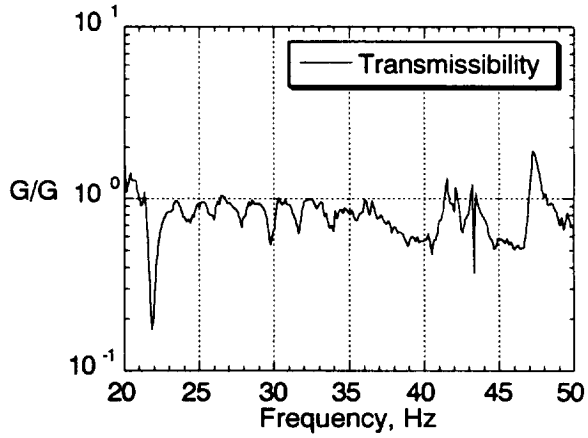

Figure 13. Isolation mount acceleration transmission

Although the payload base acceleration levels are reduced, the most important metric is the payload's boresight jitter. Outputs of the optical scoring system with and without active isolation are shown in figures 14 and 15 for two different excitations. Just using a single isolator mount provides from 50 to 80 % reduction in pointing jitter. These results are very encouraging and have led to further plans for this technology as described at the end of the next section.

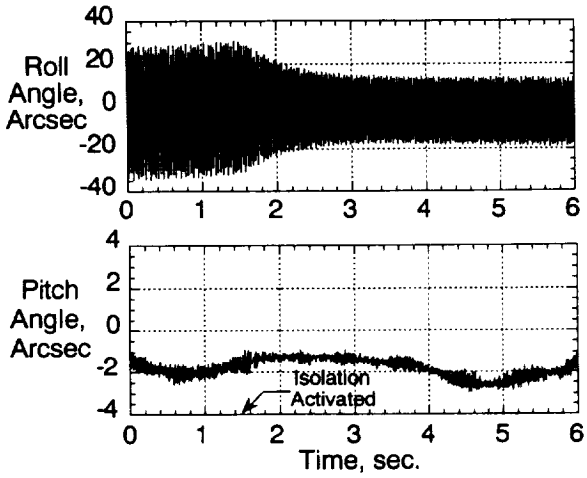

Figure 14. Payload boresight pointing, 30 Hz disturbance (isolation activated at t=1.5 sec)

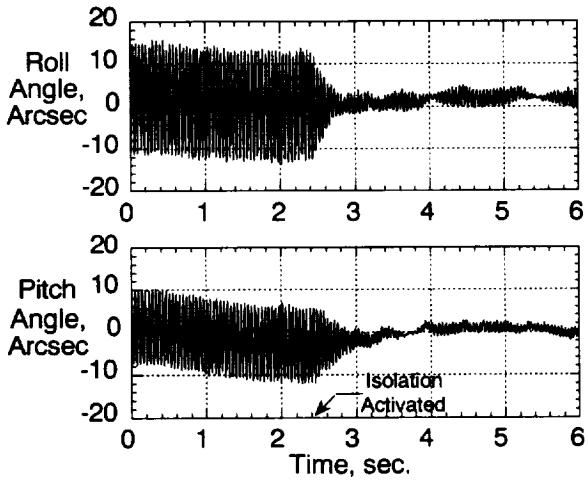

Figure 15. Payload boresight pointing, 22 Hz disturbance (isolation activated at t=2.4 sec)

Summary and Future Plans

The use of isolator mounts between science instrument payloads and the spacecraft to improve pointing performance has been discussed. These isolators can be implemented on spacecraft with relatively little impact on the existing design. Simulation of the proposed isolation technology on a real spacecraft, namely EOS AM-1, have shown up to 70 percent reduction in pointing error. Ground tests with the LaRC EOS Dynamics Testbed have confirmed 50 to 80 percent reduction in payload pointing error when active mounts are used.

By making the isolator mounts physically interchangeable with baseline kinematic mounts, a final assessment of jitter can be made as late as CDR to determine if enhanced mounts are needed to satisfy the pointing requirements. If so, an isolator mount could be incorporated with the same physical interfaces as the baseline kinematic mount at very little cost to the project.

NASA Langley is planning to develop a number of different isolation mount concepts for use in space with precision optical instruments. The objectives are to develop isolation mounts fully compatible with current instrument mount practices and capable of withstanding launch loads and the harsh space environment. Although this restricts performance and the number concepts that could be considered, it ensures minimum cost impacts to on-going programs. Plans are to examine three areas of isolator mount research and development: 1) application of new piezoelectric polymers and piezoelectric ceramics for actuation and sensing; 2) implementation of autonomous controllers to maximize adaptability of systems; 3) verification through ground testing and analytical modeling.

Currently, three instrument mount concepts are being considered which would provide one, two, or six axes of actuation. The first two concepts use flexures as their primary load carrying member. The third one is based on the concept proposed by Sirlin [23] which provides actuation in all six axes. All three concepts will be molded using recently developed piezoelectric polymers and tested to assess their capability.

Industry cooperation is being sought to provide guidance to the program and to participate in the design, fabrication, and testing of the various concepts.

Acknowledgments

The authors wish to recognize the invaluable support from their colleagues at NASA Langley. In particular, the assistance of Chris Sandridge, Peiman Maghami, Sean Kenny, and Mehzad Javeed are gratefully acknowledged. The collaborative efforts between NASA LaRC and NASA GSFC have been made possible by Jerry Newsom and Chris Scolese.

References

1. Asrar, G. and Dokken, D., editors; EOS Reference Handbook, NP-202, March 1993.

2. Rivin, E. I., "Principles and Criteria of Vibration Isolation of Machinery," *Journal of Mechanical Design*, Vol. 101 (4), Oct. 1979, pp. 682-692.

3. Tanaka, N. and Kikushima, Y., " A Study of Active Vibration Isolation," *Journal of Vibration, Acoustics, Stress, and Reliability in Design*, Vol. 107 (4), Oct. 1985, pp. 392-397.

4. Watters, B. G., Coleman, R. B., Duckworth, G. L., and Berkman, E. F.," A Perspective on Active Machinery Isolation," *Proceedings of the 27th Conference on Decision and Control*, TX., Dec. 1988, pp. 2033-2038.

5. Snowdon, J. C.," Vibration Isolation: Use and Characterization," National Bureau of Standards, Report No. NBS HB 128, May 1979.

6. Winiarz, M. L.," Liquid Spring Design Methodology for Shock Isolation System Applications," *The Shock and Vibration Bulletin, Part 3, Isolation and Damping, Vibration Test Criteria, and Vibration Analysis and Test*, pp. 17-28.

7. Rodden, J. J., Dougherty, H. J., Reschke, L. F., Hasha, M. D., and Davis, L. P., " Line-of-Sight Performance Improvement with Reaction-Wheel Isolation," *Advances in Astronautical Sciences,* 61, 1986, pp. 71-84.

8. Collins, S. A. and von Flotow, A. H., " Active Vibration Isolation for Spacecraft" *42nd Congress of the International Astronautical Federation*, Oct. 1991, Montreal, Canada, Paper No. IAF-91-289.

9. Sinha, A., Chikuan, K. K., and Grodsinsky, C. M., " A New Approach to Active Vibration Isolation for Microgravity Space Experiments," NASA TM 102470, Feb. 1990.

10. Logsdon, K., Grodsinsky, C. M. and Brown, G. M., " Development of a Vibration Isolation Prototype System for Microgravity Space Experiments," NASA TM 103664, July 1990.

11. Fenn R. and Johnson, B.," A six Degree-of-Freedom Lorentz Force Vibration Isolator with Nonlinear Controller," *International Workshop on Vibration Isolation Technology for Microgravity Science Applications*, NASA CP 10094, April 1991.

12. Boeing Defense & Space Group, Prime Item Development Specification for the Active Rack Isolation System, S684-10158, December, 1994.

13. Lurie, B. J., Fanson, J. L., and Laskin, R. A.," Active Suspensions for Vibration Isolation," *Proceedings of the 32nd AIAA/ASME/ASCE/AHS/ASC Structures, Structural Dynamics, and Materials Conference,* MD, April 1991, AIAA Paper No. 91-1232, pp. 2256-2260.

14. Blackwood, G. H. and von Flotow, A. H., "Active Vibration Isolation for Controlled Flexible Structures," MIT Space Engineering Research Center, Report No. 13-93, Oct. 1993.

15. Swanson, D. A., Miller, L. R., and Norris, M. A., " Multi-Dimensional Mount Effectiveness for Vibration Isolation," 33rd *AIAA/ASME/ASCE/AHS/ASC Structures, Structural Dynamics and Materials Conference*, TX., April 1992.

6. Maghami, P. G., Kenny, S. P., and Giesy, D. P., PLATSIM: An efficient Linear Simulation and Analysis Package for Large-Order Flexible Systems, NASA 3519, 1995.

17. Gronet, M. J., Davis, D. A., and Tan, M. K., "Development of the CSI Phase-3 Evolutionary Model Testbed," NASA Contractor Report 4630, October 1994.

18. Physik Instrumente Catalog, GmbH & Co., Waldbronn, Germany.

19. Kline, K. A., "Dynamic Analysis Using a Reduced Basis of Exact Modes and Ritz Vectors," *AIAA Journal*, Vol. 24, No. 12, December 1986, pp. 2022-2029.

20. Sandridge, C. A. and Haftka, R. T., "Modal Truncation, Ritz Vectors, and Derivatives of Closed-Loop Damping Ratios," *Journal of Guidance, Control and Dynamics*, Vol. 14, No. 4, July-August 1991, pp. 785-790.

21. Won, C. C. and Sulla, J. L., "Experiments on the Linearization of a Piezoelectric Strut," *Proceedings of the North American Conference on Smart Structures and Materials* , Vol. 2192, February 1994, pp. 168-175.

22. AD598 LVDT Signal Conditioner Product Sheet, Analog Devices, Norwood, MA.

23. Sirlin, S. W., " Vibration Isolation for Spacecraft Using the Piezo Electric Polymer PVF2," *Acoustical Society of America*, 1987.